ISSN-e: 2737-6419

Athenea Journal
Vol.5, Issue 18, (pp. 19-32)

https://doi.org/10.47460/athenea.v5i17.82

Tipo de artículo: artículo de investigación

Diagnosis of low insulation fault in the starting transient of squirrel cage rotor induction motors using wavelet analysis

Alfredo Marot
https://orcid.org/0000-0002-8829-4124
aamarotgu@estudiante.unexpo.com
Universidad de Oriente núcleo Anzoátegui
Barcelona, Venezuela

Sergio Velásquez
https://orcid.org/0000-0002-3516-4430
velasquez@unexpo.edu.ve
UNEXPO Vicerrectorado Puerto Ordaz
Puerto Ordaz, Venezuela

Correspondence author: aamarotgu@estudiante.unexpo.com

Received (12/07/2024), Accepted (15/09/2024)

Abstract. - The objective of this work was to diagnose faults in squirrel-cage induction motors during the startup transient, by analyzing the stator current signal. To achieve this, low- and medium-voltage motors were modeled in Simulink using MATLAB. Previously, the fault due to low insulation was diagnosed through a static test. It was demonstrated that, during the startup transient, the low insulation fault manifests through a Daubechies wavelet analysis at level 8 of the current signal. The fault was identified in the detail levels 1, 2, 5, 6, 7, and 8, for both low-voltage and medium-voltage motors.

Keywords: wavelet, daubechies, isolation.

Diagnóstico de falla de bajo aislamiento en el transitorio de arranque de motores de inducción con rotor jaula de ardilla mediante análisis de wavelet

Resumen: El objetivo de este trabajo fue diagnosticar fallas en motores de inducción con rotor de tipo jaula de ardilla durante el transitorio de arranque, mediante el análisis de la señal de corriente del estator. Para ello, se modelaron motores de baja y media tensión en Simulink, utilizando MATLAB. Previamente, la falla por bajo aislamiento fue diagnosticada mediante prueba estática. Se demostró que, durante el transitorio de arranque, la falla de bajo aislamiento se manifiesta a través de un análisis de wavelet Daubechies de nivel 8 aplicado a la señal de corriente. La falla se evidenció en los niveles de detalle 1, 2, 5, 6, 7 y 8, tanto en motores de baja tensión como en motores de media tensión.

Palabras clave: wavelet, daubechies, aislamiento.

I. INTRODUCTION

Induction Motors (IMs), with capacities ranging from a few watts to megawatts, are employed as prime movers and play a fundamental role in today's industries [1]. Due to their robustness, reliability, and low maintenance costs, IMs have received increasing attention in the automotive industry, electric vehicle traction, and power conversion systems [1]. Induction machines are gaining popularity in renewable energy applications, which demands constant research on their performance. The lack of regulation of failures in processes causes considerable economic losses and degrades process performance [2]. Induction motors are put to the test in a variety of circumstances and environments. Motor failure implies unwanted downtime, costly repairs, and in some cases, can even lead to casualties [3].

Motor current analysis is a valuable tool for the detection and diagnosis of faults in induction motors. This technique allows to prevent breakdowns, reduce maintenance costs, and improve the safety of facilities. Motor current signature analysis (MCSA) is considered the most common technique for fault analysis [4]. The phase current signal contains components that depend on the motor's operation, a product of the rotating flux. The appearance of faults causes changes in the supply current with specific harmonic content that depend on the type of fault. The MCSA technique uses stator current measurements to detect these harmonics, and although they are not desired, they are used for fault analysis. MCSA provides current spectra with information to detect electrical and mechanical faults. Current measurements in a three-phase induction motor can only be performed at specific times. The usual approach is to measure the current during motor operation, as it is the simplest way to do so and provides input data of sufficient quality. This technique is used by most condition monitoring methods. On-line current measurements can be divided into two types: with load and without load. Another convenient time for current signal monitoring is within the startup window [5].

Starting currents can offer better options for motor condition analysis, as they are measured at higher motor slip and with a higher signal-to-noise ratio. This facilitates the detection and evaluation of the spectral components of the signal. The most frequent causes of induction motor failures are winding and insulation problems, accounting for between 30% and 40% of total failures [6]. Insulation failures are responsible for 80 to 90% of this percentage. For medium voltage drives [7]. Stator inter-turn short circuit (ITSC), present in approximately 40% of induction motor (IM) failures, is a common defect in these machines. While a few shorted turns do not usually show any noticeable physical signs, they can cause considerable damage to the insulation in a short period of time [8]. Early detection of this fault can minimize further damage to adjacent turns and the stator core, which would reduce maintenance costs and motor downtime [9]. Most insulation faults affecting induction motors occur between phase and ground. Common practices for assessing insulation condition require the motor to be stopped and cannot provide information about the degrading agent affecting the motor [10].

An ITSC fault creates harmonic frequency components in the motor current. The magnitude and frequency of these harmonics change continuously with load variations. To accurately identify faults in induction motors (IMs), cutting-edge techniques have been developed that extract telltale features from current signals. Among the most notable tools are; Fast Fourier Transform (FFT): This technique decomposes the current signal into its frequency components, revealing unique patterns associated with different types of faults; Short Time Fourier Transform (STFT): Unlike FFT, STFT analyzes the current signal in shorter segments, providing a more detailed view of how faults evolve over time; Power Spectral Density (PSD): This technique quantifies the distribution of energy in the frequency spectrum, allowing the presence and severity of faults to be identified with greater precision. Traditional fault diagnosis techniques in induction motors, based on steady-state current, have limitations such as sensitivity to operating conditions and difficulty in detecting incipient faults. One of the most important analysis tools in both the frequency and time domains is the wavelet.

Multiresolution analysis and good time localization make wavelets very attractive for fault diagnosis research. Wavelets are localized in both the time and frequency domains because they have limited time duration and frequency bandwidth [11].

II. DEVELOPMENT

A. Mathematical model of the induction motor in the reference frame fixed to the rotor**.**

The Simulink block used in this study. implements equations that are expressed in a stationary rotor (dq) reference frame. The d axis is aligned with an axis. All quantities in the rotor reference frame are referred to the stator [12].
Equations to calculate electrical speed (ω_{em}) and sliding speed (ω_{slip}).

$$\omega_{em} = P\omega_m \quad (1)$$
$$\omega_{slip} = \omega_{sym} - \omega_{em} \quad (2)$$

To calculate the electrical speed of the rotor dq with respect to the rotor axis A (dA), the difference between the speed of the shaft and the stator is used (da) and sliding speed:

$$\omega_{dA} = \omega_{da} - \omega_{em} \quad (3)$$

o simplifies the equations for flux, voltage and current transformations, the block uses a stationary reference frame:

$$\omega_{da} = 0 \quad (4)$$
$$\omega_{dA} = -\omega_{em} \quad (5)$$

Flow

$$\begin{bmatrix}\lambda_{sd}\\ \lambda_{sq}\\ \lambda_{rd}\\ \lambda_{rq}\end{bmatrix} = \begin{bmatrix}L_s & 0 & L_m & 0\\ 0 & L_s & 0 & L_m\\ L_m & 0 & L_r & 0\\ 0 & L_m & 0 & L_r\end{bmatrix}\begin{bmatrix}I_{sd}\\ I_{sq}\\ I_{rd}\\ I_{rq}\end{bmatrix} \quad (6)$$

Current

$$\begin{bmatrix}I_{sd}\\ I_{sq}\\ I_{rd}\\ I_{rq}\end{bmatrix} = \left(\frac{1}{L_m^2 - L_r L_s}\right)\begin{bmatrix}L_s & 0 & L_m & 0\\ 0 & L_s & 0 & L_m\\ L_m & 0 & L_r & 0\\ 0 & L_m & 0 & L_r\end{bmatrix}\begin{bmatrix}\lambda_{sd}\\ \lambda_{sq}\\ \lambda_{rd}\\ \lambda_{rq}\end{bmatrix} \quad (7)$$

Inductance

$$L_s = L_{ls} + L_m \quad (8)$$
$$L_r = L_{rs} + L_m$$

Electromagnetic torque

$$T_e = PL_m(i_{sq}i_{rd} - i_{sd}i_{rq}) \quad (9)$$

Invariant power dq transformation to ensure dq and three-phase powers are equal

(10)

$$\begin{bmatrix}v_{sd}\\ v_{sq}\end{bmatrix} = \sqrt{\frac{2}{3}}\begin{bmatrix}\cos(\Theta_{da}) & \cos\left(\Theta_{da} - \frac{2\pi}{3}\right) & \cos\left(\Theta_{da} + \frac{2\pi}{3}\right)\\ -\sin(\Theta_{da}) & -\sin\left(\Theta_{da} - \frac{2\pi}{3}\right) & -\sin\left(\Theta_{da} + -\frac{2\pi}{3}\right)\end{bmatrix}\begin{bmatrix}v_a\\ v_b\\ v_c\end{bmatrix}$$

$$\begin{bmatrix}i_a\\ i_b\\ i_c\end{bmatrix} = \sqrt{\frac{2}{3}}\begin{bmatrix}\cos(\Theta_{da}) & -\sin(\Theta_{da})\\ \cos\left(\Theta_{da} - \frac{2\pi}{3}\right) & -\sin(\Theta_{da})\\ \cos\left(\Theta_{da} + \frac{2\pi}{3}\right) & -\sin(\Theta_{da})\end{bmatrix}\begin{bmatrix}i_{sd}\\ i_{sq}\end{bmatrix}$$

The equations use these variables

ω_m: Rotor angular speed (rad/s)
ω_{em}: Electric rotor speed (rad/s)
ω_{slip}: Electric rotor sliding speed (rad/s)
ω_{syn}: Synchronous rotor speed (rad/s)
ω_{da}: dq electrical speed of the stator with respect to the axis a of the rotor (rad/s)
ω_{dA}: dq electrical speed of the stator with respect to the rotor axis A (rad/s)
Θ_{da}: dq electrical angle of the stator with respect to the a axis of the rotor (rad)
Θ_{dA}: dq electrical angle of the stator with respect to the A axis of the rotor (rad)
L_q, L_d: Inductances of the q and d axes (H)
L_s: stator inductance (H)
L_r: rotor inductance (H)
L_m: Magnetizing inductance (H)
L_{ls}: Stator leakage inductance (H)
L_{lr}: Rotor leakage inductance (H)
v_{sq}, v_{sd}: Stator voltages on the q and d axes (V)
i_{sq}, i_{sd}: Stator currents in the q and d axes (A)
λ_{sq}, λ_{sd}: Stator flow in the q and d axes (Wb)
i_{rq}, i_{rd}: Rotor currents in the q and d axes (A)
λ_{rq}, λ_{rd}: Rotor q and d axis flow (Wb)
v_a, v_b, v_c: Stator voltage phases a, b, c (V)
i_a, i_b, i_c: Stator currents phases a, b, c (A)
R_s: Resistance of stator windings (Ohm)
R_r: Rotor winding resistance (Ohm)
P: Number of pole pairs
T_e: electromagnetic torque (Nm)

A. Wavelet transforms

The wavelet transform (WT) is a signal analysis technique that solves the time-frequency resolution problems of the Fourier transform. The WT is based on a function called the wavelet mother function, which is used to decompose the signal into sub-bands. Wavelet functions can be classified into families, and the choice of the appropriate family depends on the characteristics of the signal to be studied. The most used wavelet functions are Daubechies, coiflet, simlet, biorthogonal and discrete Meyer. [13].

Identification of the fault can be done in two ways: by analyzing the coefficients resulting from the decomposition of the signal or by studying the high-level wavelet signals. High-level wavelet signals are those that contain information about the nature of the failure. The integral wavelet transforms of a function f(t) ϵ L^2 with respect to a wavelet analyzer Ø is defined as [14]:

$$W_\psi f(a,b) = \int_{-\infty}^{\infty} f(t)\psi_{b,a}(t)\,dt \tag{11}$$

Where

$$\psi_{b,a}(t) = \frac{1}{\sqrt{a}}\psi\frac{t-b}{a} \qquad a > 0 \tag{12}$$

The parameters b and a are called translation and dilation parameters respectively. Normalization factor is included $\sqrt{a}$ so that $\|\psi_{b,a}\| = \|\psi\|$

The expression for the inverse wavelet transform is

$$f(t) = \frac{1}{C_\psi}\int_{-\infty}^{\infty} db \int_{-\infty}^{\infty} \frac{1}{a^2}[W_\psi f(b,a)]\psi_{b,a}(t)da \quad (13)$$

Where $C_\emptyset$ is a constant that depends on the choice of the wavelet and is given by:

$$C_\psi = \int \frac{|\hat{\psi}(\omega)|}{|\omega|} d\omega < \infty \quad (14)$$

The coefficients constitute the results of a regression of the original signal carried out on the wavelets. A graph can be generated with the x-axis representing the position along the signal (time), the y-axis representing the scale, and the color at the x-y point representing the magnitude of the wavelet coefficient C. These coefficient plots are generated with graphic tools.

A. Discrete Wavelet Transform (DWT)

The discrete wavelet transform performs the decomposition of a signal $x[n]$ in an approximation coefficient at a given level of decomposition $k, A_k[n]$, and k detail signs$d_j[n]$ con $j = 1 \dots k$ [15].

$$x[n] = A_k[n] + \sum_{j=1}^{k} d_j[n] = \sum_i \Phi_i^k[n] + \sum_{j=1}^{k}\sum_i d_i^j \Psi_i^j[n] \quad (15)$$

Where Φ^k y Ψ^j They are the scaling function at level k and the wavelet function at level j respectively. On the other hand, the coefficients a_i^k y d_i^jse calculan utilizando el algoritmo de codificación por sub-bandas [16].

Discrete Wavelet Coiflet $B_k = (-1)^k C_{N-1-k}$ (16)

Wavelet Cohen Daubechies $B_k = (-1)^k C_{N-1-k}$ (17)

Wavelet Daubechies $B_k = (-1)^k C_{N-1-k}$ (18)

Binomial-quadrature mirror filter (QMF) $h(n) = \sum_{r=0}^{n-2/2} \theta_r X_r(n)$ (19)

Wavelet Haar $\psi_{n,k} = \psi(2^n t - k)$ (20)

Wavelet Mathieu $H_v(\omega) = -e^{-jv\omega/2}\frac{ce_v(\omega/2, q)}{ce_v(0,q)}$ (21)

Wavelet Legendre $H_v(\omega) = 1/\sqrt{2}\sum_{k\epsilon Z} h^v e^{-j\omega k}$ (22)

III. METHODOLOGY

In this work we start from the fact that we have proposed the following hypothesis:

Hypothesis: The hypothesis posits that Wavelet analysis using Daubechies wavelets applied to squirrel-cage induction motors will effectively detect and diagnose insulation faults, considering the specific motor properties that influence the dynamics of these faults. A significant relationship is expected between the individual characteristics of the studied motors and the Wavelet analysis' ability to accurately and timely identify existing insulation faults, which will contribute to improving predictive maintenance practices in industrial machinery.

Study Population and Sample: The study population consisted of 477 electric motors from a petrochemical plant with a history of low insulation problems in some motors. A sample of 20 motors with data from previous static insulation tests was available. The objective was to employ wavelet analysis to evaluate these motors and demonstrate its ability to diagnose low insulation faults.

Motor Simulations: In this scenario, 20 squirrel-cage induction motors were simulated in Simulink. For this study, one low-voltage and one medium-voltage motor were selected. The low-voltage motor belonged to a process fluid pump in the Urea plant, and the medium-voltage motor belonged to a pump in the plant's cooling water system. These motors were chosen because the low-voltage motor was the most recent one subjected to a static insulation test, and the insulation resistance value obtained was less than 200 kΩ, which is below the value established in IEEE Standard 43-2013 (5 MΩ between phases and ground and between phases for low-voltage motors). The medium-voltage motor was selected because it was one of the highest-power motors in the population, allowing the proposed methodology to be validated for medium-voltage motors as well.

Taking into consideration that if a ground fault is introduced in phase C of the motors, modeling the insulation resistance of the winding. Starting from the fact that; You can emulate the insulation resistance to ground by connecting a resistor to ground for each coil [17]. So to emulate insulation deterioration, a capacitor is added, which increases the insulation capacitance.

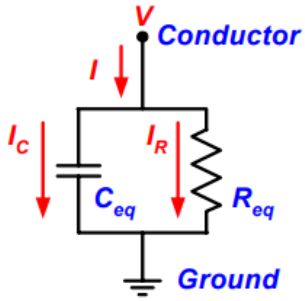

Fig. 1. Equivalent circuit of electrical insulation system [18].

Modeling the circuit in figure 1

$$I_c(t) + I_R(t) = I(t) \tag{23}$$

$$\frac{C_{eq}dv(t)}{dt} + \frac{V(t)}{R_{eq}} = I(t) \tag{24}$$

This approach was chosen because an aged insulating material would also cause a similar increase in capacitance. The severity of insulation degradation can be varied depending on the capacitance of the inserted capacitor. Phase to ground capacitances are between 1.5 nF and 21 nF [19]. The "3-phase induction motor" block from the Simscape Electrical library in Simulink was used. To model each engine individually. The parameters of each engine were configured according to the actual specifications or available reference data. In which we can obtain the data required by the software, below we show the data of the low voltage model motor.

Nominal Voltage (Vn) = 460;
Nominal frecuency (fn) = 60;
Rated Current (In) = 18.25;
Nominal Torque (Tn) = 49,8;
Maximum speed (Ns) = 1800;
Nominal speed (Nn) =1750;
Starting Current to Rated Current Ratio (Ist/In) = 6;
Starting Torque to Nominal Torque Ratio (Tst/Tn) = 2.5;

Breaking Torque to Nominal Torque Ratio (Tbr/Tn) = 3;
power factor (pf)= 0.8;

With these data we introduce them into the parameter estimation block;

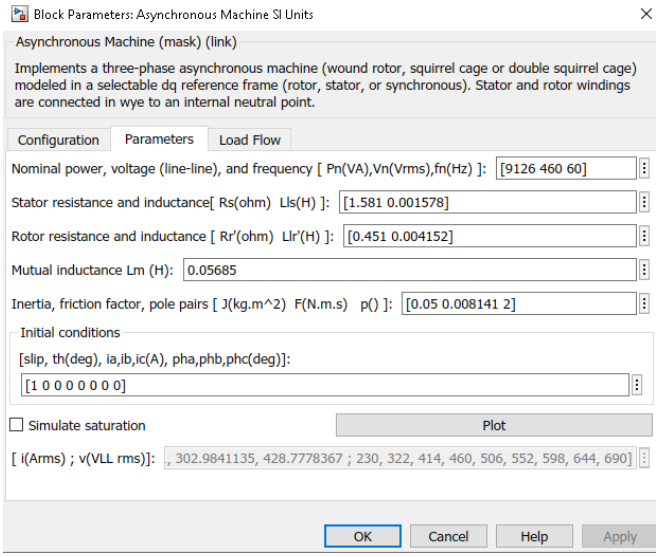

Fig. 2. Parameters of Low Voltage Motor 460 V, 11 KW; simulated in simulink.

The C phase current signal is extracted and brought into MATLAB to perform a wavelet analysis. Using the "3-Phase Induction Motor" block from the Simscape Electrical library in Simulink to model each motor.

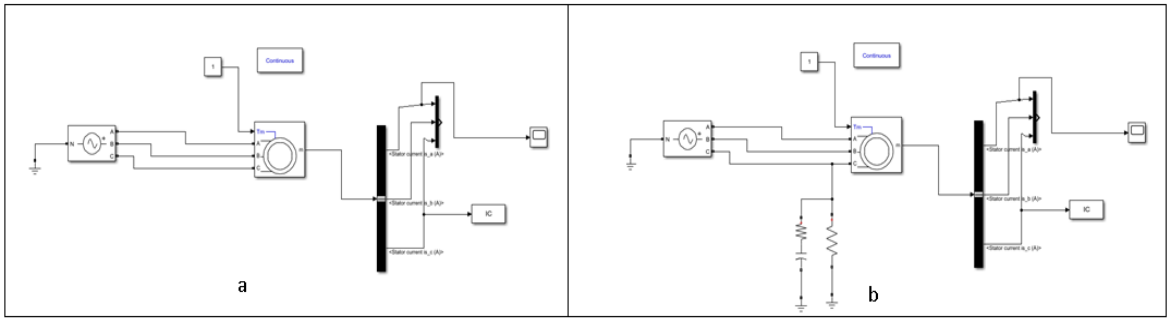

Fig. 3. Low and medium squirrel cage motor simulation; healthy state (a). Low and medium squirrel cage motor simulation; Insulation failure (b)

The simulation of the start-up of the two induction machines in a healthy state was carried out. Subsequently, the current signal of the start transient of phase C was extracted, with the Simulink Workspace block into Matlab, for the healthy and failed cases. The signal was transferred from the Simulink workspace to MATLAB for wavelet analysis using the level 8 Daubechies parent function.

IV. RESULTS

The results of the simulation of the start-up of the induction machines revealed a change in the signal at all levels of detail; but more pronounced at the level of detail 1, 2, 5, 7 and 8; from Daubechies wavelet analysis. In the spectrum, the modification of both signals can be observed for both the medium voltage motor and the low voltage motor. Figure 5 shows the decomposition of the wavelet signal at level 8 in the healthy state of the engine.

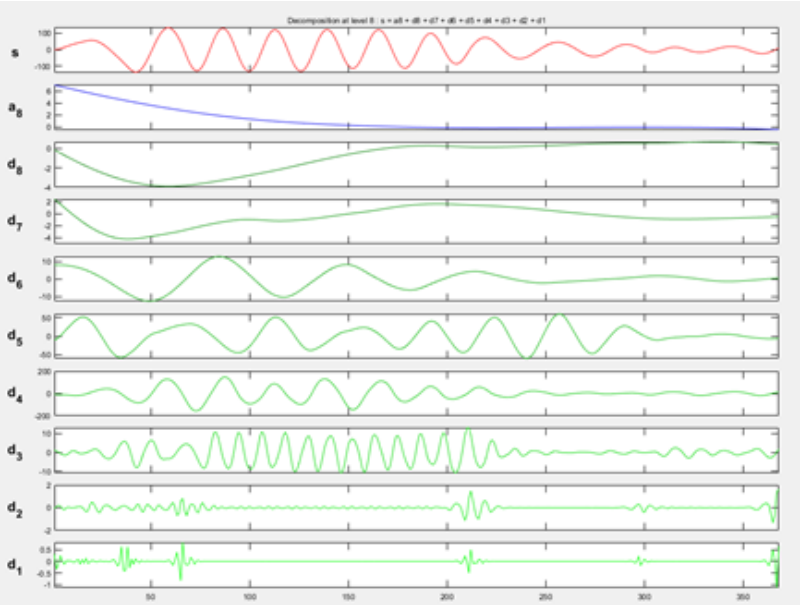

Fig. 4. Wavelet Daubechies Level 8 Low Voltage Motor 460 V, 11 KW; shows the spectrum of the engine in healthy state.

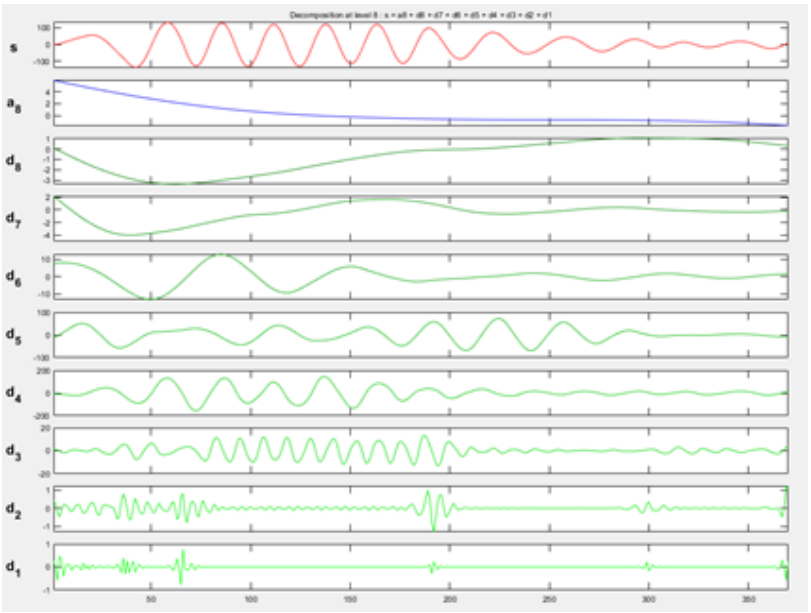

Fig. 5. Wavelet Daubechies Level 8 Low Voltage Motor 460 V, 11 KW; shows the spectrum of the motor in the fault state with low insulation.

Figure 4 shows the decomposition of the wavelet signal at level 8 in the healthy state of the engine. When viewing both spectra, we can observe the difference that exists with respect to figure 5 at the level of detail Daubechies 1, 2, 3, 5, 7 and 8; how the signal changes when a 200kΩ low insulation fault is introduced.

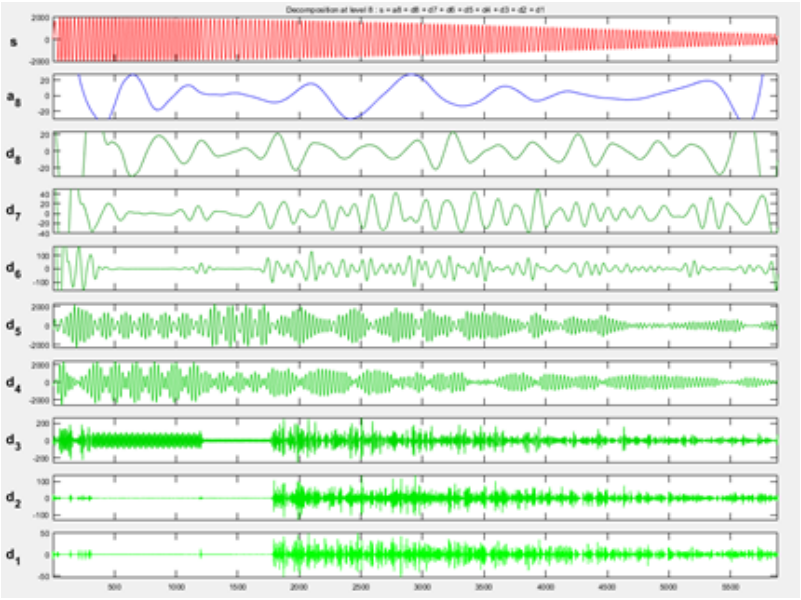

Fig. 6. Wavelet Daubechies Level 8 Medium Voltage Motor 13800 V, 3 MVA; shows the spectrum of the engine in healthy state.

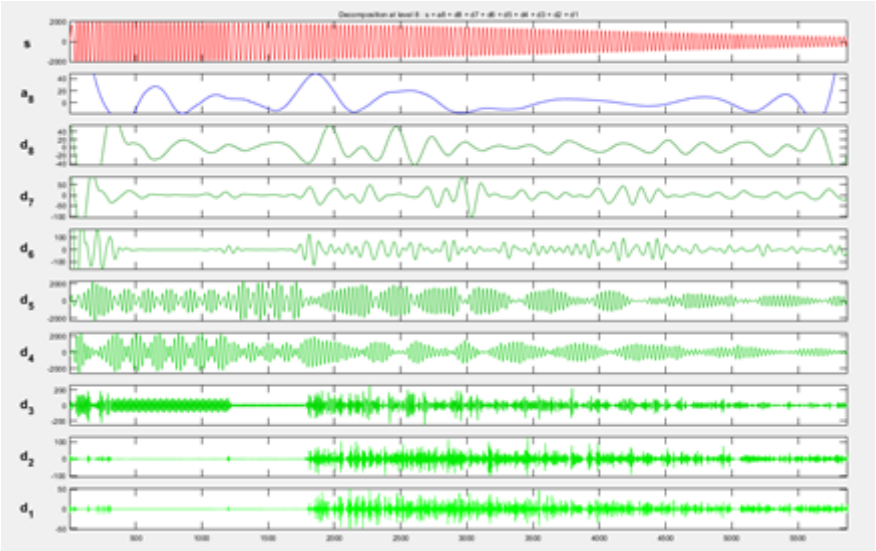

Fig. 7. Wavelet Daubechies Level 8 Medium Voltage Motor 13800 V, 3 MVA; shows the spectrum of the motor with insulation failure for 200kΩ.

Figure 7. Wavelet Daubechies Level 8 Medium Voltage Motor 13800 V, 3 MVA; simulated in simulink; shows the spectrum of the engine in healthy state. Figure 8; Wavelet Daubechies Level 8 Medium Voltage Motor; We can observe the difference with respect to figure 7 in the level of detail Daubechies 8, 7 and 6 in this case as the signal changes when a low insulation fault of 200kΩ is introduced.

Next we analyze wavelet histograms which can show how wavelet coefficients are distributed at different scales. In this case, they are used to analyze the health status of low and medium voltage motors, both in healthy conditions and with failure due to low insulation.

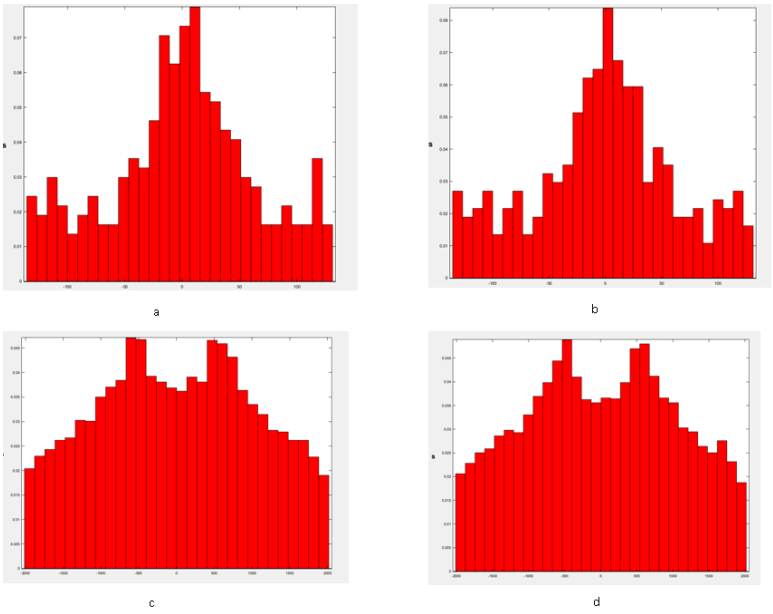

Fig. 9. Histograms. Wavelet Daubechies Level 8 Medium and low voltage motor.

Figure 9 shows Histograms. Wavelet Daubechies Level 8 Medium and low voltage motor. The first top left histogram (a) belongs to the low voltage motor in healthy state, the second top right side histogram (b) belongs to the motor in failed state with low insulation. The lower left side histogram (c) belongs to the medium voltage motor in healthy state. The lower right-side histogram (c) belongs to the failed medium voltage motor with low insulation. The histograms of the low voltage motor represent a significant difference in the distribution of energy levels, both have a unimodal distribution, but the one in the failed state is more asymmetric than that of the motor in the healthy state, with a longer tail to the right. . This may indicate a greater tendency towards higher wavelet coefficient values, which could be related to low insulation failure. The histograms of the medium voltage motor present a bimodal distribution, and a difference is made in terms of the peaks on the left side with two almost uniform bands in the case of the healthy motor. The medium voltage healthy state histogram is slightly asymmetric to the right, similar to that of the low voltage motor in healthy state.

In the case of the low voltage motor, we have then simulated 2 low insulation scenarios; in which it could be detected that as the insulation degrades at 20 kΩ and 2 kΩ; You can continue to observe the changes in the levels of detail of the wavelet spectrum, in addition to the energy distribution changing in the signal; In Table 1 we can observe the changes in the statistics of the signal energy distribution for each scenario, motor in healthy state, failed motor with 200 kΩ, 20 kΩ and 2 kΩ;

Table 1. the statistics of the signal energy distribution.

Statistical	Healthy	Isolation 200k	Isolation 20k		Isolation 2k
mean	-0,3463	-1,011	-0,7334		-0,7312
median	2,347	0,8336	1,93		1,966
miximum	131,2	131,5	131,4		131,4
minimum	-135,6	-135,3	-135,6		-135,6
range	266,9	266,9	267		167
standard dev	63,46	63,4	63,24		63,24
median abs dev	36,6	39,91	38,96		39,89
mean abs dev	49,62	49,47	49,41		49,42
l1 norm	1,83E+04	1,83E+04	1,82E+04		1,82E+04
L2 norm	1216	1220	1215		1215
max norm	135,6	135,3	135,6		135,6

IEEE Standard 493 provides valuable information on expected failure rates for high-power electric motors. According to this standard, a differentiation in failure rates is observed depending on the operating voltage and the type of motor:Motores de inducción:

Less than 1000 Volts: The estimated failure rate is 0.0824. From 1000 to 5000 Volts: The estimated failure rate is 0.0714 [20]. Taking this reference for our population at this failure rate, it is likely that in a year we will have 32 low voltage motors and 7 medium voltage motors. Therefore, it would be estimated that of the 31 low voltage motors, taking the reference mentioned above, 40% of the failures will be due to winding problems. We include in these problems generated by insulation failures; With this probability, 13 low voltage motors and 7 medium voltage motors would fail, so to validate the tests we carried out simulations taking these samples as a reference.

We wish to evaluate whether the diagnosis of failure due to low insulation of electric motors using Daubuchies 8 wavelet transform signal analysis at level 8 is effective to identify failures in low voltage motors. There is data from a sample of 13 low voltage motors, where 12 motors were correctly diagnosed as failed. The failure rate of low voltage motors provided by the IEEE (0.0824) and the EPRI estimate of the proportion of failures due to insulation problems (40%) are taken as a reference. Hipótesis:

Null hypothesis (H0): Diagnosis by wavelet transform has no effect on the identification of faults due to low isolation, that is, the probability of a correct diagnosis is not different from the random probability.

Alternative hypothesis (H1): Diagnosis by wavelet transform does have an effect on the identification of faults due to low isolation, that is, the probability of a correct diagnosis is greater than the random probability. (We work under the assumption that this hypothesis is correct).

Statistical test selection:

Since we are trying to evaluate the proportion of correct diagnoses in a small sample (n < 30), the student's t test for a single sample can be used.

Calculation of the test statistic:

Number of successes (X): 12 engines diagnosed as failed (of 13 engines in the sample).
Population means under the null hypothesis (μ0): 0.4, since it is estimated that 40% of the motors are failed due to low insulation.

Sample standard deviation (s): It is calculated using the formula:

$$s = \sqrt{\frac{(\sum x_i - \mu_0)^2}{(n-1)}} \tag{25}$$

In this case, s = 0.241.

test statistic t:

$$t = \frac{(X - \mu_0)}{\left({}^{s}/_{\sqrt{n}}\right)} = \frac{(12 - 0{,}4)}{\left({}^{0{,}241}/_{\sqrt{12}}\right)} = 2{,}49 \tag{26}$$

Degrees of freedom:

$$gl = n - 1 = 13 - 1 = 12 \tag{27}$$

Significance level:

A significance level (α) of 0.05 is established.

Calculation of p value:

Since this is a right-sided test, the p-value is calculated using Student's t-table with 12 degrees of freedom and finding the area in the tail of the test statistic t = 2.49. In this case, the p value is 1.782 in table.

$$t_{exp} > t_{tab}$$

The null hypothesis is rejected and the alternative hypothesis is accepted. This means that there is sufficient evidence to conclude that the Daubechies wavelet diagnostic method does have a significant effect on the identification of low insulation faults in low voltage electric motors.

CONCLUSIONS

Daubechies Level 8 Wavelet analysis is presented as a novel and effective tool for diagnosing low insulation faults in the stator coils of squirrel cage rotor induction motors, both at low and medium voltage. This technique, based on the analysis of the stator current signal during the start-up transient, allows low insulation faults to be accurately identified through characteristic changes in the wave spectrum and energy distribution of the current signals. Levels of detail 8, 7, 6 and 5 are particularly relevant for the detection of these faults. The detail curve patterns vary significantly in the failed engine with respect to the healthy engine. The wavelet histograms show a difference in the distribution of energy levels between the healthy and the failed motor, indicating a greater tendency towards higher wavelet coefficient values in the failed motor. The student's t test for a single sample demonstrates that wavelet transform diagnosis does have a significant effect on the identification of faults due to low insulation in low voltage electric motors. Unlike traditional static-state insulation testing, Daubechies Level 8 Wavelet Analysis offers early and accurate fault detection, even in the presence of low insulation values. This capability opens a promising path for the implementation of the method in condition monitoring systems, improving predictive maintenance practices and reducing the incidence of catastrophic failures in electric motors. This study provides strong evidence supporting Daubechies Level 8 wavelet analysis as a valuable tool for the diagnosis and prevention of low insulation faults in induction motors.

REFERENCES

[1] A. Almounajjed, A. Sahoo y M. Kumar, «Condition monitoring and fault diagnosis of induction motor: An experimental analysis,» de In 2021 7th Int. Conf. on Electrical . In 2021 7th Int. Conf. on Electrical, 2021.

[2] X. Liang, M. Z. Ali y H. Zhang, «Induction Motors Fault Diagnosis Using Finite Element Method: A Review,» in IEEE Transactions on Industry Applications, vol. 56, nº 2, pp. 1205-1217, 2020.

[3] P. Zitha y B. A. Thango, «On the Study of Induction Motor Fault Identification using Support Vector Machine Algorithms,» de 2023 SAUPEC Conference, Johannesburg, South Africa, 2023.

[4] A. Sharma, L. Mathew y S. Chatterji, «Analysis of Broken Rotor bar Fault Diagnosis for Induction Motor. In Proceedings of the,» de IEEE International Conference on Innovations in Control, Communication and Information Systems (ICICCI),, Greater Noida, 2017.

[5] M. R. Mehrjou, N. Mariun, M. H. Marhaban y N. Misron, «Rotor fault condition monitoring techniques for squirrel-cage induction machine—A review,» Mechanical Systems and Signal Processing, vol. 25, nº 8, pp. 2827-2848, 2011.

[6] M. Z. Ali, S. M. N. S. K, X. Liang y H. Y. Zhang and T, «Machine Learning-Based Fault Diagnosis for Single- and Multi-Faults in Induction Motors Using Measured Stator Currents and Vibration Signals,» in IEEE Transactions on Industry Applications, vol. 5, nº 3, pp. 2378-2391, 2019.

[7] S. Lee, J. Yang, K. Younsi y R. Bharadwaj, «An On-line Groundwall and Phase to Phase Insulation Quality Assessment Technique for AC Machine Stator Windings,» IEEE Transactions on Industry Applications, vol. 42, p. 946–957, 2006.

[8] Y. Wang, L. Yang, J. Xiang y e. al, «A hybrid approach to fault diagnosis of roller bearings under variable speed conditions,» Measurement Science and Technology, vol. 28, nº 12, 2017.
[9] G. H. Bazan, P. R. Scalassara, W. Endo y e. al, «Stator short-circuit diagnosis in induction motors using mutual information and intelligent systems,» IEEE Transactions on Industrial Electronics, vol. 66, nº 4, pp. 3237-3246, 2018.
[10] A.S.Guedes y S.M.Silva, «Insulation Protection and Online Stress Agent Identification for Electric Machines using Artificial Intelligence,» ET Electric Power Applications, vol. 13, nº 4, pp. 559-570 , 2019.
[11] G. Mathew, «Fault Detection in an Induction Motor Drive Using Discrete Wavelet Packet Transform,» IOSR Journal of Electrical and Electronics Engineering (IOSR-JEEE), vol. 12, nº 2, pp. 1-6, 2017.
[12] N. Mohan, Advanced Electric Drives: Analysis, Control and Modeling Using Simulink. Minneapolis, Minneapolis: MNPERE, 2001.
[13] J. Antonino-Daviu, M.-F. J. Riera-Guasp, F. Martínez-Giménez y A. Peris, «Application and optimization of the discrete wavelet transform for the detection of broken rotor bars in induction machines,» Applied and Computational Harmonic Analysis, vol. 21, nº 2, pp. 268-279, 2006.
[14] J. Cusidó y J. Romeral, «Transient Analysis and Motor Fault Detection using the Wavelet Transform,» MCIA Group, Technical University of Catalonia, pp. 43-60, 2011.
[15] J. Walker, CRC press, 2008.
[16] R. Gopinath y G. H.ta, Introduction to wavelets and wavelet transforms: a primer, Nueva Jersey: Prentice-Hall, 1997.
[17] M. Samiullah, H. Ali y A. A. Shehryar Zahoor, «Fault Diagnosis on Induction Motor using Machine Learning and Signal Processing,» School of Electrical Engineering and Computer Science, (SEECS), National University of Sciences and Technology, pp. 1-6, 2024.
[18] K. Younsi, P. Neti, M. Shah, J. Y. Zhou, J. Krahn y K. Weeber, «On-line Capacitance and Dissipation Factor Monitoring of AC Stator Insulation,» IEEE Transactions on Dielectrics and Electrical Insulation , vol. 17, nº 5, pp. 1441-1451, 2010.
[19] P. Nussbaumer, M. A. Vogelsberger y T. M. Wolbank, «Induction Machine Insulation Health State Monitoring Based on Online Switching Transient Exploitation,» IEEE TRANSACTIONS ON INDUSTRIAL ELECTRONICS, vol. 62, nº 3, pp. 1835- 1845, 2015.
[20] I. o. E. a. E. E. (IEEE), IEEE 493-2020: Recommended Practice for the Design of Relays for Electric Power Systems., 2020.

THE AUTHORS

Alfredo Alejandro Marot Guevara; Electrical/Electronic Engineer, specialist in Industrial Automation and Computing; University professor for 18 years. Currently professor of Dynamic Systems at the Universidad de Oriente, advisor at MDJ Technology. c.a; and SJT Industrial Equipment and Services, residing in the city of Barcelona, Anzoátegui. Venezuela.

Sergio Rafael Velásquez Guzmán - Coauthor, received the B.S. degree in Electronic Engineering, from the UNEXPO, in 2008. M.S. degree in Education from UPEL in 2011, an M.S. degree in Electronic Engineering from UNEXPO, in 2012, an MBA degree from UNY in 2014, a Doctor of Education degree in 2015 from UPEL, and a Doctor of Engineering Sciences from UNEXPO in 2019. He is a type B Research Professor accredited by the MINCYT in Venezuela. Currently, he is in charge of the Research and Postgraduate Department of the UNEXPO Vice-Rectorate, Puerto Ordaz, Venezuela.